

# Reinterpretation and Extension of Entropy Correction Terms for Residual Distribution and Discontinuous Galerkin Schemes

Rémi Abgrall, Philipp Öffner, Hendrik Ranocha\*

13th August 2019

For the general class of residual distribution (RD) schemes, including many finite element (such as continuous/discontinuous Galerkin) and flux reconstruction methods, an approach to construct entropy conservative semidiscretisations by adding suitable correction terms has been proposed recently by Abgrall (J. Comp. Phys. 372: pp. 640–666, 2018). Here, these correction terms are characterised as solutions of certain optimisation problems and adapted to discontinuous element based schemes such as discontinuous Galerkin and (multi-block) finite difference methods. Novel generalisations to entropy inequalities, multiple constraints, and kinetic energy preservation for the Euler equations are developed and tested in numerical experiments. Finally, the underlying idea to use optimisation problems is applied to grid refinement and coarsening operators, resulting in entropy stable/dissipative grid transfers.

**Key words.** entropy stability, kinetic energy preservation, conservation laws, residual distribution schemes, discontinuous Galerkin schemes, Euler equations

**AMS subject classification.** 65M12, 65M60, 65M70, 65M06

## 1 Introduction

Consider a hyperbolic conservation law

$$\partial_t u(t, x) + \sum_{j=1}^d \partial_j f^j(u(t, x)) = 0, \quad t \in (0, T), x \in \Omega, \quad (1)$$

---

\*Corresponding author.

in  $d$  space dimensions such as the compressible Euler equations of gas dynamics, where  $u: (0, T) \times \Omega \rightarrow \Upsilon \subseteq \mathbb{R}^m$  are the conserved variables,  $f^j: \Upsilon \rightarrow \mathbb{R}^m$  the fluxes, and  $t \in (0, T)$ ,  $x \in \Omega \subseteq \mathbb{R}^d$  the time and space coordinates, respectively. Of course, the conservation law has to be equipped with appropriate initial and boundary conditions.

Given a convex entropy  $U: \Upsilon \rightarrow \mathbb{R}$  and entropy fluxes  $F^j: \Upsilon \rightarrow \mathbb{R}$  fulfilling  $\partial_u U \cdot \partial_u f^j = \partial_u F^j$ , smooth solutions of (1) satisfy  $\partial_t U(u) + \sum_{j=1}^d \partial_j F^j(u) = 0$  and the entropy inequality

$$\partial_t U(u) + \sum_{j=1}^d \partial_j F^j(u) \leq 0 \quad (2)$$

is used as additional admissibility criterion for weak solutions, cf. [10]. Because of the convexity of  $U$ , the entropy variables  $w = \partial_u U$  and the conservative variables  $u$  can be used interchangeably.

Ever since the seminal work of Tadmor [38], there has been some interest in techniques to mimic (2) for semidiscretisations of hyperbolic conservation laws. Some recent contributions are, e.g. [7–9, 16, 28, 35, 40]. Recently, relaxation Runge–Kutta methods have been proposed to transfer such semidiscrete entropy conservation/dissipation results to fully discrete schemes [22, 31].

In this article, the correction terms enforcing entropy conservation of numerical methods in the general class of residual distribution (RD) schemes proposed by Abgrall [2] and modifications suggested in [27] are studied deeper. They are characterised as solutions of certain optimisation problems and different weightings are introduced. Additionally, new applications and generalisations are developed and compared in numerical experiments. Finally, the basic idea of such an optimisation approach is applied to grid refinement and coarsening, resulting in entropy stable/dissipative transfer operations.

This article is structured as follows. Firstly, the numerical schemes and entropy correction terms are introduced in Section 2, starting with residual distribution schemes in Section 2.1. Thereafter, discontinuous element based schemes such as discontinuous Galerkin (DG) methods are described in Section 2.2 and the characterisations of entropy correction terms as solutions of certain optimisation problems are developed. Generalisations to entropy inequalities, multiple linear constraints, and kinetic energy preservation for the compressible Euler equations are developed in Section 3. Numerical examples using all these schemes are presented in Section 4. Next, the application of such optimisation ideas to grid refinement and coarsening is developed in Section 5, including numerical examples. Finally, the results of this study are summed up in Section 6, conclusions are drawn and some directions of further research are presented.

## 2 Entropy Corrections for Numerical Schemes

In this section, existing formulations of entropy correction terms for residual distribution and discontinuous element based schemes are described and an interpretation in terms of a quadratic minimisation problem is presented.

## 2.1 Nodal Formulation: Residual Distribution Schemes

The first introductions of residual distribution (RD) schemes, also denoted by fluctuation splitting schemes, can be found in Roe's seminal work [33] and in the paper by Ni [23]. Since then, further developments have been done for generalisation and to reach high order in the discretisation, cf. [2, 4] and references therein. The main advantage of the RD approach is the abstract formulation of the schemes. One works only with the degrees of freedom (DoFs). The selection of approximation/solution space and the definition of the residuals specifies the scheme completely and thus the properties of the considered methods. Today, the RD ansatz provides a unifying framework including some — if not most — of the up-to-date used high order methods like continuous and discontinuous Galerkin methods and flux reconstruction schemes [2, 5]. Also the schemes which will be considered in Section 2.2 can be recast into this framework. However, to follow the approach of Abgrall [2], where the entropy correction term is introduced for the first time, the same notation and the general RD approach is applied which will be shortly repeated in the following subsection.

### Residual Distribution Schemes

For simplicity, we will explain the RD approach only for the steady state problem

$$\sum_{j=1}^d \partial_j f^j(u(x)) = 0, \quad x \in \Omega, \quad (3)$$

of a hyperbolic conservation law (1) with suitable boundary conditions. RD is applied to discretise (3) in space. A discretisation of (3) will be considered and the correction term is working on this. A possible temporal discretisation for time-dependent problems will be not considered in the following part. Several time-integration methods such as deferred correction and Runge–Kutta schemes to discretise (1) fully together with an RD approach can be found in [1, 3, 32] and references therein, but this is not topic of this paper.

The domain  $\Omega$  is split into subdomains  $\Omega_l$  (e.g. triangles in two dimensions). The term  $K$  denotes the generic element of the mesh and  $h$  is used for the characteristic mesh size. For the boundary elements,  $\Gamma$  is applied. Then, the degrees of freedom  $\sigma$  (DoFs) are defined in respect to the splitting and the weights in each  $K$ . For each  $K$ , the set of DoFs  $\Sigma_K$  of linear forms acting on the set  $\mathbb{P}^k$  of polynomials of degree  $k$  such that the linear mapping  $q \in \mathbb{P}^k \mapsto (\sigma_1(q), \dots, \sigma_{|\Sigma_K|}(q))$  is one-to-one and  $\mathcal{S}$  denotes the set of degrees of freedom in all elements.

The solution  $u$  will be approximated by an element from the space  $\mathcal{V}^h$  defined as

$$\mathcal{V}^h := \bigoplus_K \left\{ u^h \in L^2(K), u^h|_K \in \mathbb{P}^k \right\}. \quad (4)$$

A linear combination of basis functions  $\varphi_\sigma \in \mathcal{V}^h$  will be used to describe the numerical

solution

$$u^h(x) = \sum_{K \in \Omega_l} \sum_{\sigma \in K} u_\sigma^h \varphi_\sigma|_K(x), \quad \forall x \in \Omega, \quad (5)$$

where the coefficients  $u_\sigma^h$  must be found by a numerical method. Therefore, the residuals come finally into play. Now, the RD scheme can be formulated by the following three steps to calculate the coefficients  $u_\sigma^h$ , which are also illustrated in Figure 1:

1. Define for any  $K$  the total residual<sup>1</sup>  $\Phi^K$  of (3) as an approximation of

$$\Phi^K \approx \int_K \sum_{j=1}^d \partial_j f^j(u^h). \quad (6)$$

In the following,  $\oint$  will be used to denote the discrete evaluation of integrals by some quadrature rule. For continuous Galerkin schemes, one can choose

$$\Phi^K = \oint_K \sum_{j=1}^d \partial_j f^j(u^h). \quad (7)$$

Other examples are given in [2] and in Example 2.3 below.

2. Split the total residual into sub-residual  $\Phi_\sigma^K$  for each degree of freedom  $\sigma \in K$ , so that the sum of all the contributions over an element  $K$  is the fluctuation term itself, i.e.

$$\Phi^K = \sum_{\sigma \in K} \Phi_\sigma^K, \quad \forall K. \quad (8)$$

3. The resulting scheme is finally obtained by summing all sub-residuals of one degree of freedom from different elements  $K$ , i.e.

$$\sum_{K \mid \sigma \in K} \Phi_\sigma^K = 0, \quad \forall \sigma. \quad (9)$$

The term (9) allows to calculate the coefficients  $u_\sigma^h$  in the numerical approximation (5).

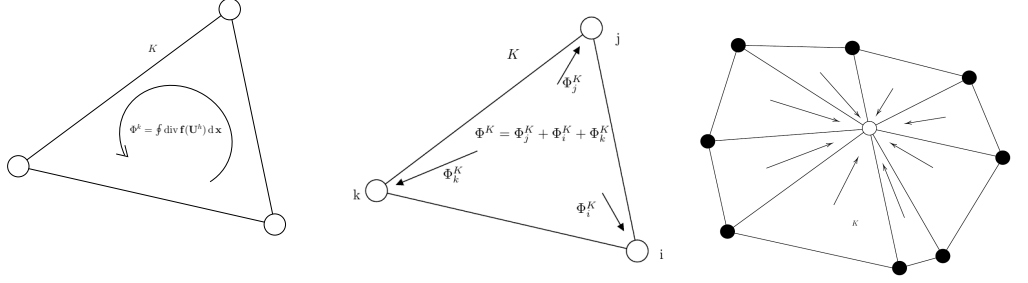
If  $\sigma \in \Gamma$ , equation (5) will be split for any DoF and we can finally write the discretisation of (3) as

$$\sum_{K \in \Omega} \sum_{\sigma \in K} \Phi_\sigma^K(u^h) + \sum_{\Gamma \in \partial\Omega} \sum_{\sigma \in \Gamma} \Phi_\sigma^\Gamma(u^h) = 0, \quad (10)$$

where  $\Phi_\sigma^\Gamma$  denotes the boundary residual. With (10) the RD scheme is described. To specify completely the method (FV, DG, etc.), the solution space (4) (and therefore also the basis) has to be chosen and the exact definition of the residuals  $\Phi_\sigma^K$  has to be given.

---

<sup>1</sup>This term is also referred as fluctuation term in the literature [6].



(a) Step 1: Compute the total residual. (b) Step 2: Split the total residual. (c) Step 3: Combine the residuals.

Figure 1: Illustration of the three steps (total residual, nodal residuals, gathering residuals) of the RD approach for linear triangular elements.

Varying selections yield different methods. However, the conservation relation has to be always fulfilled. For any element  $K$  and any  $u^h \in \mathcal{V}^h$ ,

$$\sum_{\sigma \in K} \Phi_{\sigma}^K(u^h) = \oint_{\partial K} f^{\text{num},j} \left( u_{|K}^h, u_{|K^-}^h \right) \cdot v_j, \quad (11)$$

where  $u_{|K}^h$  is the restriction of  $u^h$  in the element  $K$ ,  $u_{|K^-}^h$  is the restriction of  $u^h$  on the other side of the local edge/face of  $K$ , and  $v_j$  is the  $j$ -th component of the outer unit normal vector  $v$  at  $\partial K$ . In addition,  $f^{\text{num}}$  is a consistent numerical flux, i.e.  $f^{\text{num},j}(u, u) = f^j(u)$ , and summation over repeated indices is implied. Similar equations (11) hold for the boundary residuals, see [2] for details.

Further properties of the scheme can be written in terms of the residuals. Here, the focus lies on the reinterpretation and extension of the entropy correction term introduced in [2].

### Entropy Correction Term

In [2], the author presented an approach to construct entropy conservative/stable schemes in a general framework. Therefore, a correction term is added to the scheme  $\Phi_{\sigma}^K$  at every degree of freedom  $\sigma \in K$  to ensure that the scheme fulfills discretely the entropy condition (2). In terms of RD, an entropy conservative scheme<sup>2</sup> fulfills

$$\sum_{\sigma \in K} \left\langle w_{\sigma}, \tilde{\Phi}_{\sigma}^K \right\rangle = \oint_{\partial K} F^{\text{num},j} \left( w_{|K}^h, w_{|K^-}^h \right) v_j, \quad (12)$$

where  $F^{\text{num},j}$  is a numerical entropy flux and  $w_{\sigma}$  is the entropy variable at the Dof  $\sigma$ .

---

<sup>2</sup>An entropy stable semidiscretisation has an inequality in (2). Here, the steady state case (3) is considered.

In addition, these correction terms have to be chosen such that they do not violate the conservation relation. The correction term  $r_\sigma^K$  is added to the residual  $\Phi_\sigma^K$  at every degree of freedom, such that the corrected residual

$$\tilde{\Phi}_\sigma^K = \Phi_\sigma^K + r_\sigma^K \quad (13)$$

fulfils the discrete entropy condition (12). In [2], the following correction term is introduced

$$r_\sigma^K = \alpha(w_\sigma - \bar{w}), \quad \text{with } \bar{w} = \frac{1}{\#K} \sum_{\sigma \in K} w_\sigma, \quad (14)$$

$$\alpha = \frac{\mathcal{E}}{\sum_{\sigma \in K} (w_\sigma - \bar{w})^2}, \quad \mathcal{E} := \oint_{\partial K} F^{\text{num},j} \left( w_K^h, w_{|K^-}^h \right) v_j - \sum_{\sigma \in K} \langle w_\sigma, \Phi_\sigma^K \rangle. \quad (15)$$

**Theorem 2.1.** *If the constraints to not contradict each other, the correction term (14) with (15) satisfies*

$$\sum_{\sigma \in K} r_\sigma^K = 0, \quad \sum_{\sigma \in K} \langle w_\sigma, r_\sigma^K \rangle = \mathcal{E}. \quad (16)$$

By adding (14) to the residual  $\Phi_\sigma^K$ , the resulting scheme using  $\tilde{\Phi}_\sigma^K$  is locally conservative in  $u$  and entropy conservative.

*Proof.* The relation (16) defines a linear system of equation with always at least two unknowns. It is enough to show that (14) with (15) is a valid solution. Results concerning possible contradictions of the constraints (16) are given below in Remark 2.6.

The conservation relation for the new scheme is guaranteed because of

$$\begin{aligned} \sum_{\sigma \in K} r_\sigma^K &= \sum_{\sigma \in K} \alpha(w_\sigma - \bar{w}) = \alpha \left( \sum_{\sigma \in K} w_\sigma - \sum_{\sigma \in K} \left( \frac{1}{\#K} \sum_{\sigma \in K} w_\sigma \right) \right) \\ &= \alpha \left( \sum_{\sigma \in K} w_\sigma - \sum_{\sigma \in K} w_\sigma \right) = 0. \end{aligned} \quad (17)$$

The entropy condition is satisfied, since

$$\begin{aligned} \sum_{\sigma \in K} \langle w_\sigma, r_\sigma^K \rangle &= \sum_{\sigma \in K} \langle w_\sigma, \alpha(w_\sigma - \bar{w}) \rangle = \alpha \sum_{\sigma \in K} \langle w_\sigma, (w_\sigma - \bar{w}) \rangle \\ &= \alpha \sum_{\sigma \in K} \langle w_\sigma - \bar{w}, w_\sigma - \bar{w} \rangle + \underbrace{\left\langle \bar{w}, \sum_{\sigma \in K} (w_\sigma - \bar{w}) \right\rangle}_{=0} = \frac{\mathcal{E}}{\sum_{\sigma \in K} (w_\sigma - \bar{w})^2} \sum_{\sigma \in K} (w_\sigma - \bar{w})^2 = \mathcal{E}. \end{aligned} \quad (18)$$

It is obvious that  $\tilde{\Phi}_\sigma^K$  fulfils the entropy condition (12).  $\square$

**Remark 2.2.** The error behaviour of  $\mathcal{E}$  can be controlled through the used numerical quadrature, see [2] for details.

To finish this section, an example describing a specific scheme will be presented.

**Example 2.3.** To express a discontinuous Galerkin scheme in the RD framework, one has to specify the solution space and the residual in detail. The space  $\mathcal{V}^h$  is given by (4) and the residual is given by

$$\Phi_\sigma^K(u^h) = - \oint_K \partial_j \varphi_\sigma \cdot f^j(u^h) + \oint_{\partial K} \varphi_\sigma f^{\text{num},j}(u_{|K}^h, u_{|K^-}^h) \cdot \nu_j. \quad (19)$$

The boundary residuals are

$$\Phi_\sigma^\Gamma(u^h) = \oint_\Gamma \nabla \varphi_\sigma \left( f^{\text{num},j}(u_{|\Gamma}^h, u_b) - f^j(u^h) \cdot \nu_j \right). \quad (20)$$

## 2.2 Operator Formulation: Discontinuous Element Based Schemes

Here, the focus will lie on element based discretisations using an operator formulation as in [27]. Therefore, the domain  $\Omega$  is partitioned into non-overlapping elements  $\Omega_l \subseteq \Omega$  and the following discrete operators are used on each element (dropping the elemental index  $l$  for convenience).

- A symmetric and positive definite mass matrix  $M$ , approximating the  $L^2$  scalar product via  $\int_{\Omega_l} u(x)v(x)dx = \langle u, v \rangle_{L^2} \approx \langle u, v \rangle_M = u^T M v$ .
- Derivative matrices  $D_j$ , approximating the partial derivative  $\partial_j u \approx D_j u$ .
- A restriction/interpolation operator  $R$ , performing interpolation to the boundary nodes at  $\partial\Omega_l$  via  $Ru$ .
- A symmetric and positive definite boundary mass matrix  $B$ , approximating the scalar product on  $L^2(\partial\Omega_l)$ .
- Multiplication operators  $N_j$ ,  $j \in \{1, \dots, d\}$ , representing the multiplication of functions on the boundary  $\partial\Omega_l$  by the  $j$ -th component  $\nu_j$  of the outer unit normal  $\nu$  at  $\partial\Omega_l$ .

Together, the restriction and boundary operators approximate the boundary integral with respect to the outer unit normal as in the divergence theorem, i.e.

$$u^T R^T B N_j R v \approx \int_{\partial\Omega} u \nu \nu_j. \quad (21)$$

If the SBP property

$$M D_j + D_j^T M = R^T B N_j R \quad (22)$$

is fulfilled, integration by parts (the divergence theorem) is mimicked on a discrete level, cf. [12]. For example, some discontinuous Galerkin schemes can be formulated in this way [18], allowing the transfer of stability results established at the continuous level to the discretisation, cf. [13, 36] and references cited therein.

The general semidiscretisations considered here can be written as

$$\partial_t u = \text{VOL} + \text{SURF}, \quad (23)$$

where VOL are volume terms discretising  $\partial_j f^j(u)$  and SURF are surface terms implementing interface/boundary conditions weakly. For the  $i$ -th conserved variable  $u_i$ ,  $i \in \{1, \dots, m\}$ , the corresponding semidiscretisation is

$$\partial_t u_i = \text{VOL}_i + \text{SURF}_i. \quad (24)$$

**Example 2.4.** A central nodal DG scheme using the numerical (surface) fluxes  $f^{\text{num},j}$  can be obtained by choosing

$$\text{VOL} = -D_j f^j, \quad \text{SURF} = -M^{-1} R^T B N_j (f^{\text{num},j} - R f^j). \quad (25)$$

**Example 2.5.** A flux differencing or split form discretisation using symmetric numerical volume fluxes  $f^{\text{vol},j}$  and numerical surface fluxes  $f^{\text{num},j}$  can be obtained using [14, 19]

$$\text{VOL}^{(m)} = -2 \sum_{j=1}^d \sum_k D_{j,m,k} f^{\text{vol},j}(u^{(m)}, u^{(k)}), \quad \text{SURF} = -M^{-1} R^T B N_j (f^{\text{num},j} - R f^j), \quad (26)$$

where the upper indices  $(m), (k)$  indicate the grid node. Examples using such a notation can be found in [26, 28, 30] and references cited therein.

The discretisation should be (locally) conservative, i.e. it should satisfy

$$\forall i \in \{1, \dots, m\} : \quad 1^T M \partial_t u_i = -1^T R^T B N_j f_i^{\text{num},j}, \quad (27)$$

where  $f_i^{\text{num},j}$  is the numerical flux for the  $i$ -th conserved variable in coordinate direction  $j$ . An entropy conservative semidiscretisation results in

$$w_i^T M \partial_t u_i = -1^T R^T B N_j F^{\text{num},j}, \quad (28)$$

where a summation over the repeated index  $i$  is implied and  $F^{\text{num},j}$  are numerical entropy fluxes corresponding to  $f^{\text{num},j}$ , cf. [37, 38].

The basic idea of Abgrall [2] is to enforce (28) for any semidiscretisation via the addition of a correction term  $r$  that is consistent with zero and does not violate the conservation relation (27), resulting in

$$\partial_t u_i = \text{VOL}_i + \text{SURF}_i + r_i. \quad (29)$$

Using the mass matrix  $M$  for discrete integration as proposed in [27], the correction term is

$$\begin{aligned} \mathbf{r}_i &= \alpha \left( \mathbf{w}_i - \frac{\mathbf{1}^T M \mathbf{w}_i}{\mathbf{1}^T M \mathbf{1}} \mathbf{1} \right), \quad \alpha = \frac{\mathcal{E}}{\mathbf{w}_k^T M \mathbf{w}_k - \frac{(\mathbf{1}^T M \mathbf{w}_k)(\mathbf{1}^T M \mathbf{w}_k)}{\mathbf{1}^T M \mathbf{1}}}, \\ \mathcal{E} &= -\mathbf{1}^T R^T B N_j F^{\text{num},j} - \mathbf{w}_k^T M \text{VOL}_k - \mathbf{w}_k^T M \text{SURF}_k. \end{aligned} \quad (30)$$

If the denominator of  $\alpha$  in (30) is zero, the numerical solution is constant in the element because of the Cauchy Schwarz inequality (since  $\mathbf{1}$  and  $\mathbf{w}_k$  are linearly dependent for each  $k$  in that case). Then, the discontinuous element scheme reduces to a finite volume scheme using the numerical fluxes  $f^{\text{num},j}$  and (28) has to hold for entropy conservative numerical fluxes  $f^{\text{num},j}$ , as described in the following Remark 2.6. Additionally, the term multiplied by  $\alpha$  vanishes and  $\mathbf{r}$  becomes zero.

**Remark 2.6.** Such a correction is only possible, if the constraints (27) and (28) do not contradict each other. In particular, (28) has to hold whenever all  $w_i$  are constant (proportional to 1). This is satisfied for the schemes investigated in this section, if the numerical surface fluxes  $f^{\text{num},j}$  are entropy conservative and  $F^{\text{num},j}$  the corresponding numerical entropy fluxes in the sense of Tadmor [37, 38], i.e. if

$$(w_{i,+} - w_{i,-}) f_i^{\text{num},j} (w_-, w_+) = \psi_+^j - \psi_-^j, \quad (31)$$

$$F^{\text{num},j} = \frac{w_{i,+} + w_{i,-}}{2} f_i^{\text{num},j} (w_-, w_+) - \frac{\psi_+^j + \psi_-^j}{2}, \quad (32)$$

where  $\psi^j$  is the flux potential  $\psi^j = w_i f_i^j - F^j$ . Indeed, if the numerical solution is constant in an element, DG type schemes such as in Example 2.6 result in a finite volume scheme

$$\partial_t u = -M^{-1} R^T B N_j (f^{\text{num},j} - R f^j), \quad (33)$$

which is conservative because of  $\mathbf{1}^T R^T B N_j R f^j = 0$  (since the divergence theorem has to hold for constants because of consistency). Additionally,

$$\begin{aligned} w_i^T M \partial_t u_i &= -w_i^T R^T B N_j f_i^{\text{num},j} + w_i^T R^T B N_j R f_i^j \\ &= -w_i^T R^T B N_j f_i^{\text{num},j} + \mathbf{1}^T R^T B N_j R \psi^j. \end{aligned} \quad (34)$$

Hence, it suffices to consider one boundary node. There,

$$\begin{aligned} \psi_{\pm}^j - w_{i,\pm} f_i^{\text{num},j} (w_-, w_+) &= \psi_{\pm}^j - \left( \frac{w_{i,+} + w_{i,-}}{2} \pm \frac{w_{i,+} - w_{i,-}}{2} \right) f_i^{\text{num},j} (w_-, w_+) \\ &= \psi_{\pm}^j - \frac{w_{i,+} + w_{i,-}}{2} f_i^{\text{num},j} (w_-, w_+) \mp \frac{\psi_+^j - \psi_-^j}{2} \\ &= \frac{\psi_+^j + \psi_-^j}{2} - \frac{w_{i,+} + w_{i,-}}{2} f_i^{\text{num},j} (w_-, w_+) = -F^{\text{num},j}. \end{aligned} \quad (35)$$

**Theorem 2.7.** *If  $\mathcal{E} = 0$  whenever all  $w_i$  are constant, the correction term  $\mathbf{r}$  (30) is the unique optimal correction of (29), measured in the discrete norm induced by  $M$ , such that (27) and (28) are satisfied, i.e.  $\mathbf{r} = (\mathbf{r}_1, \dots, \mathbf{r}_m)$  (30) is the unique solution of*

$$\min_{\mathbf{r}} \frac{1}{2} \|\mathbf{r}\|_M^2 \quad \text{s. t. } \mathbf{1}^T M \mathbf{r}_i = 0, \quad w_i^T M \mathbf{r}_i = \mathcal{E}, \quad (36)$$

where  $\|\mathbf{r}\|_M^2 = \mathbf{r}_i^T M \mathbf{r}_i$ .

*Proof.* Equation (36) can be reformulated as

$$\min_{\mathbf{r}} \frac{1}{2} \mathbf{r}^T (\mathbf{I}_m \otimes M) \mathbf{r} \quad \text{s. t. } A \mathbf{r} = b, \quad A = \begin{pmatrix} \mathbf{I}_m \otimes (1^T M) \\ w_i^T (\mathbf{I}_m \otimes M) \end{pmatrix}, \quad b = \begin{pmatrix} 0 \\ \mathcal{E} \end{pmatrix}. \quad (37)$$

Since  $M$  is symmetric and positive definite, there is a unique solution  $\mathbf{r}$ , which is given by [24, Section 16.1]

$$\begin{pmatrix} (\mathbf{I}_m \otimes M) & -A^T \\ A & 0 \end{pmatrix} \begin{pmatrix} \mathbf{r} \\ \lambda \end{pmatrix} = \begin{pmatrix} 0 \\ b \end{pmatrix} \quad (38)$$

for some  $\lambda \in \mathbb{R}^{m+1}$ . Hence,  $\mathbf{r}$  must satisfy the  $m+1$  constraints  $\mathbf{1}^T M \mathbf{r}_i = 0$ ,  $w_i^T M \mathbf{r}_i = \mathcal{E}$  and  $M \mathbf{r}_i$  must be in the span of  $\{M \mathbf{1}, M w_i\}$  such that the coefficients of  $M w_i$  are the same for all  $i \in \{1, \dots, m\}$ . This is obviously true for  $\mathbf{r}_i$  as defined in (30).  $\square$

Using the same argument used in the proof of Theorem 2.7, one obtains

**Proposition 2.8.** *If  $\mathcal{E} = 0$  in (15) whenever  $w$  is constant in  $K$ , the correction term  $r_\sigma^K$  (14) is the unique optimal correction of (13), measured in the discrete norm induced by the identity matrix  $\mathbf{I}$ , such that (12) and  $\sum_{\sigma \in K} r_\sigma^K = 0$  are satisfied, i.e.  $\mathbf{r} = (r_\sigma^K)_\sigma$  (14) is the solution of*

$$\min_r \frac{1}{2} \|r\|_{\mathbf{I}}^2 \quad \text{s. t. } \mathbf{1}^T \mathbf{I} r_\sigma^K = 0, \quad w_\sigma^T \mathbf{I} r_\sigma^K = \mathcal{E}, \quad (39)$$

where  $\|r\|_{\mathbf{I}}^2 = (r_\sigma^K)^T \mathbf{I} r_\sigma^K$ .

**Remark 2.9.** There are some differences between the role of the correction terms  $\mathbf{r}_i$  described in this section and the terms  $r_\sigma^K$  used in the previous section. Firstly, since the correction  $\mathbf{r}_i$  (30) is added to the other side of the hyperbolic equation, the sign differs from the correction term  $r_\sigma^K$  (14) of [2]. Secondly,  $\mathbf{r}_i$  (30) is a correction for the pointwise time derivative of  $u$  while  $r_\sigma^K$  (14) is a correction for an integrated version. Loosely speaking, they are related via

$$r_\sigma^K \simeq M \mathbf{r}_i. \quad (40)$$

Additionally, the role of the indices differs:  $\mathbf{r}_i$  is a correction term for the  $i$ -th variable at all grid nodes while  $r_\sigma^K$  is a correction term at the grid node  $\sigma$  for all variables (if a DG type setting is used for the RD scheme).

**Remark 2.10.** Using the notation of this section, the correction term  $r_\sigma^K$  (14) of [2] corresponds to

$$\begin{aligned} \mathbf{r}_i &= \alpha \left( M^{-1} \mathbf{w}_i - \frac{\mathbf{1}^T \mathbf{w}_i}{\mathbf{1}^T \mathbf{1}} M^{-1} \mathbf{1} \right), \quad \alpha = \frac{\mathcal{E}}{\mathbf{w}_k^T \mathbf{w}_k - \frac{(\mathbf{1}^T \mathbf{w}_k)(\mathbf{1}^T \mathbf{w}_k)}{\mathbf{1}^T \mathbf{1}}}, \\ \mathcal{E} &= \mathbf{1}^T \mathbf{R}^T \mathbf{B} \mathbf{N}_j \mathbf{F}^{\text{num},j} - \mathbf{w}_k^T \Phi_k. \end{aligned} \quad (41)$$

While  $r_\sigma^K$  (14) is the optimal correction with respect to the identity matrix, its corresponding pointwise correction  $\mathbf{r}_i$  (41) is optimal with respect to the norm induced by  $M^2$ .

**Remark 2.11.** Using the notation of RD schemes, the entropy correction term  $\mathbf{r}_i$  (30) corresponds to

$$\begin{aligned} r_\sigma^K &= \alpha \left( \oint_K w_\sigma \varphi_\sigma - \frac{\sum_{\varrho \in K} \oint_K w_\varrho \varphi_\varrho}{\sum_{\varrho \in K} \oint_K \varphi_\varrho} \oint_K \varphi_\sigma \right) = \alpha \left( w_\sigma - \frac{\sum_{\varrho \in K} \oint_K w_\varrho \varphi_\varrho}{\sum_{\varrho \in K} \oint_K \varphi_\varrho} \right) \oint_K \varphi_\sigma, \\ \alpha &= \frac{-\oint_{\partial K} \mathbf{F}^{\text{num},j} (w_{|K}^h, w_{|K^-}^h) \nu_j + \sum_{\sigma \in K} \langle w_\sigma, \Phi_\sigma^K \rangle}{\sum_{\sigma, \varrho \in K} \oint_K |w_\sigma|^2 \varphi_\sigma - \frac{1}{\oint_K 1} \left( \sum_{\sigma \in K} \oint_K (w_\sigma \varphi_\sigma) \right) \cdot \left( \sum_{\varrho \in K} \oint_K (w_\varrho \varphi_\varrho) \right)}, \end{aligned} \quad (42)$$

in accordance with (40). Hence, (30) uses an integral weighting (by the quadrature rule) instead of a summation without weights. While  $\mathbf{r}_i$  (30) is the optimal correction with respect to the mass matrix  $M$ , its corresponding integral correction  $r_\sigma^K$  (42) is optimal with respect to the norm induced by  $M^{-1}$ .

### 2.3 Finite Difference and Global Spectral Collocation Schemes

Classical single block finite difference and spectral collocation schemes can be interpreted as RD or DG schemes described in Sections 2.1 and 2.2 with one element. In that case, the entropy corrections described above yield globally conservative and globally entropy conservative/stable schemes.

Sadly, global conservation and a global entropy inequality do not imply any sort of convergence towards an entropy solution of scalar conservation laws, even if the scheme converges.

**Example 2.12.** Consider Burgers' equation

$$\begin{aligned} \partial_t u(t, x) + \partial_x \frac{u(t, x)^2}{2} &= 0, \quad t > 0, x \in [0, 3], \\ u(0, x) &= u_0(x), \quad x \in [-2, 2], \end{aligned} \quad (43)$$

with periodic boundary conditions and the initial condition

$$u_0(x) = \begin{cases} -1, & \text{if } 1 < x < 2, \\ +1, & \text{else.} \end{cases} \quad (44)$$

The unique entropy solution contains a stationary shock at  $x = 1$  and a rarefaction wave starting at  $x = 2$ .

Central periodic finite difference and Fourier collocation schemes can be represented by a skew-symmetric derivative operator  $D$  and mass matrix  $M \propto I$ . Hence, there is no difference between the approaches (14) and (30).

Since  $u^2$  is constant, a classical central scheme yields a stationary numerical solution. The entropy correction vanishes, too, since  $\mathcal{E}$  is zero (because of periodic boundary conditions). Hence, the same stationary numerical solution is obtained if the entropy correction is added.

If an element based scheme is used instead, the numerical solution with entropy correction term cannot be stationary if the grid is fine enough (obtained by increasing the number of elements), since the difference of numerical entropy boundary fluxes does not vanish if the element contains exactly one initial discontinuity.

## 2.4 Related Schemes

By Theorem 2.7, the entropy correction terms can be interpreted as solution of a quadratic minimisation problem with equality constraints. The idea of solving such a problem can also be exploited for many different applications.

**Remark 2.13.** A similar approach has been used in [20] to construct entropy conservative numerical fluxes. In their work, the authors focus on the quadratic optimization problem

$$\min_{f^{\text{num}}} \frac{1}{2} \left\| f^{\text{num}} - \bar{f} \right\|_{\hat{M}^{-1}}^2 \quad \text{s. t. } [[w]]^T f^{\text{num}} = [[\psi]], \quad (45)$$

where  $[[\cdot]]$  denotes the jump and  $\psi$  is the flux potential. The function  $\bar{f}$  denotes any symmetric and consistent numerical flux and  $f^{\text{num}}$  is the new (symmetric) entropy conservative numerical flux.

**Remark 2.14.** The approach using a quadratic optimisation problem can be extended to more general constraints that are linear for a given state  $u$ , e.g. some special form of the kinetic energy for the Euler equations, cf. Section 3.3. A combination of split forms and correction terms similar to the ones described hitherto has been presented in [34].

## 3 Generalisations

In this section, some generalisations of the entropy correction terms based on the interpretations as a quadratic optimisation problem will be developed. Here, the notation of Section 2.2 for discontinuous element based schemes will be used.

### 3.1 Inequality Constraints

In many applications to hyperbolic conservation laws, the main interest lies in an entropy *inequality* instead of entropy conservation, resulting in some kind of stability estimates.

For example, even if the baseline scheme is not necessarily entropy dissipative in general, it can be dissipative in some cases. In that case, it could be beneficial to preserve this dissipation introduced by the baseline scheme. Moreover, it could be possible to obtain better approximations with smaller corrections if some entropy dissipation is allowed. Instead of (36) in Theorem 2.7, such an optimisation problem is

$$\min_{\mathbf{r}} \frac{1}{2} \|\mathbf{r}\|_M^2 \quad \text{s. t. } \mathbf{1}^T M \mathbf{r}_i = 0, \quad w_i^T M \mathbf{r}_i \leq \mathcal{E}. \quad (46)$$

While a solution of (46) is still conservative, i.e. (27) holds, the entropy inequality

$$w_i^T M \partial_t u_i \leq -\mathbf{1}^T R^T B N_j F^{\text{num},j} \quad (47)$$

holds instead of the entropy equality (28).

**Theorem 3.1.** *If the constraints do not contradict each other, the optimisation problem (46) has a unique solution  $\mathbf{r}$ , which is given by  $\mathbf{r} = 0$  if  $\mathcal{E} > 0$  and (30) if  $\mathcal{E} \leq 0$ .*

*Proof.* Since  $M$  is symmetric and positive definite, there is a unique solution. Apply the active set method described in [24, Section 16.4] with feasible initial value of  $\mathbf{r}$  given in (30) to

$$\min_{\mathbf{r}} \frac{1}{2} \|\mathbf{r}\|_M^2 \quad \text{s. t. } \mathbf{1}^T M \mathbf{r}_i = 0, \quad -w_i^T M \mathbf{r}_i \geq -\mathcal{E}. \quad (48)$$

Since (30) solves the optimisation problem (36), the sign of the Lagrange multiplier associated with  $-w_i^T M \mathbf{r}_i \geq -\mathcal{E}$  determines the next step:

- If the Lagrange multiplier is  $\geq 0$ , the unique solution has been found.
- Otherwise, drop the constraint  $-w_i^T M \mathbf{r}_i \geq -\mathcal{E}$  and compute the solution of

$$\min_{\mathbf{r}} \frac{1}{2} \|\mathbf{r}\|_M^2 \quad \text{s. t. } \mathbf{1}^T M \mathbf{r}_i = 0, \quad (49)$$

which is obviously  $\mathbf{r} = 0$ .

Finally, note that the Lagrange multiplier associated with  $-w_i^T M \mathbf{r}_i \geq -\mathcal{E}$  is  $-\alpha$ , where  $\alpha$  is given in (30) and satisfies  $\text{sign}(\alpha) = \text{sign}(\mathcal{E})$ .  $\square$

**Remark 3.2.** Theorem 3.1 simply states that the semidiscretisation (29) obtained by the correction solving (46) is given by the unmodified method if it is entropy dissipative and by the entropy conservative scheme (30) if the baseline scheme produces spurious entropy (per element).

### 3.2 Multiple Linear Constraints

A generalisation of the approach described in Theorem 2.7 to multiple linear constraints is straightforward. This is demonstrated for two constraints

$$w_i^T M \mathbf{r}_i = \mathcal{E}, \quad \tilde{w}_i^T M \mathbf{r}_i = \tilde{\mathcal{E}} \quad (50)$$

in addition to (27). Here,  $\tilde{\mathcal{E}}$  is the difference of desired and current values for a linear constraint similar to  $\mathcal{E}$  in (30). For example,  $\tilde{\mathcal{E}}$  could be caused by a correction for the kinetic energy for the Euler equations, cf.  $\mathcal{E}$  in (66) below.

**Theorem 3.3.** *If the constraints (27) and (50) do not contradict each other, the unique solution  $\mathbf{r} = (\mathbf{r}_1, \dots, \mathbf{r}_m)$  of*

$$\min_{\mathbf{r}} \frac{1}{2} \|\mathbf{r}\|_M^2 \quad \text{s. t. } 1^T M \mathbf{r}_i = 0, \quad w_i^T M \mathbf{r}_i = \mathcal{E}, \quad \tilde{w}_i^T M \mathbf{r}_i = \tilde{\mathcal{E}}, \quad (51)$$

is given by

$$\mathbf{r}_i = \alpha \left( w_i - \frac{1^T M w_i}{1^T M 1} 1 \right) + \tilde{\alpha} \left( \tilde{w}_i - \frac{1^T M \tilde{w}_i}{1^T M 1} 1 \right), \quad (52)$$

where

$$\begin{pmatrix} \alpha \\ \tilde{\alpha} \end{pmatrix} = \begin{pmatrix} w_i^T M w_i - \frac{(1^T M w_i)(1^T M w_i)}{1^T M 1} 1 & w_i^T M \tilde{w}_i - \frac{(1^T M w_i)(1^T M \tilde{w}_i)}{1^T M 1} 1 \\ \tilde{w}_i^T M w_i - \frac{(1^T M \tilde{w}_i)(1^T M w_i)}{1^T M 1} 1 & \tilde{w}_i^T M \tilde{w}_i - \frac{(1^T M \tilde{w}_i)(1^T M \tilde{w}_i)}{1^T M 1} 1 \end{pmatrix}^{-1} \begin{pmatrix} \mathcal{E} \\ \tilde{\mathcal{E}} \end{pmatrix}. \quad (53)$$

*Proof.* Equation (51) can be reformulated as

$$\min_{\mathbf{r}} \frac{1}{2} \mathbf{r}^T (I_m \otimes M) \mathbf{r} \quad \text{s. t. } A \mathbf{r} = b, \quad A = \begin{pmatrix} I_m \otimes (1^T M) \\ w^T (I_m \otimes M) \\ \tilde{w}^T (I_m \otimes M) \end{pmatrix}, \quad b = \begin{pmatrix} 0 \\ \mathcal{E} \\ \tilde{\mathcal{E}} \end{pmatrix}. \quad (54)$$

As in the proof of Theorem 2.7,  $\mathbf{r}$  must satisfy the constraints  $1^T M \mathbf{r}_i = 0, w^T M \mathbf{r} = \mathcal{E}, \tilde{w}^T M \mathbf{r}_i = \tilde{\mathcal{E}}$  and  $M \mathbf{r}_i$  must be in the span of  $\{M 1, M w_i, M \tilde{w}_i\}$  such that the coefficients of  $M w_i$  and  $M \tilde{w}_i$  are the same for all  $i \in \{1, \dots, m\}$ , respectively. Hence,

$$\mathbf{r}_i = \alpha w_i + \tilde{\alpha} \tilde{w}_i + c_i, \quad (55)$$

where

$$\begin{aligned} 1^T M \mathbf{r}_i = 0 &\iff \alpha 1^T M w_i + \tilde{\alpha} 1^T M \tilde{w}_i + c_i 1^T M 1 = 0 \\ &\iff c_i = -\frac{\alpha 1^T M w_i + \tilde{\alpha} 1^T M \tilde{w}_i}{1^T M 1}. \end{aligned} \quad (56)$$

Finally,  $\alpha$  and  $\tilde{\alpha}$  have to solve

$$\begin{aligned} \left( w_i^T M w_i - \frac{(1^T M w_i)(1^T M w_i)}{1^T M 1} \right) \alpha + \left( \tilde{w}_i^T M \tilde{w}_i - \frac{(1^T M \tilde{w}_i)(1^T M \tilde{w}_i)}{1^T M 1} \right) \tilde{\alpha} &= \mathcal{E}, \\ \left( \tilde{w}_i^T M w_i - \frac{(1^T M \tilde{w}_i)(1^T M w_i)}{1^T M 1} \right) \alpha + \left( \tilde{w}_i^T M \tilde{w}_i - \frac{(1^T M \tilde{w}_i)(1^T M \tilde{w}_i)}{1^T M 1} \right) \tilde{\alpha} &= \tilde{\mathcal{E}}, \end{aligned} \quad (57)$$

proving the assertion.  $\square$

**Remark 3.4.** It can be desirable to satisfy entropy (in-) equalities for multiple entropies. Based on Remark 2.6, the numerical surface fluxes  $f^{\text{num},j}$  should be entropy conservative for both entropies. However, this is in general not possible. Indeed, for a scalar conservation law and a fixed entropy, the entropy conservative numerical flux is uniquely determined as

$$f^{\text{num},j} = \frac{\llbracket \psi^j \rrbracket}{\llbracket w \rrbracket}. \quad (58)$$

### 3.3 Kinetic Energy for the Euler Equations

Consider the compressible Euler equations in two space dimensions (the extension to three space dimensions is straightforward)

$$\underbrace{\partial_t \begin{pmatrix} \varrho \\ \varrho v_x \\ \varrho v_y \\ \varrho e \end{pmatrix}}_{=u} + \underbrace{\partial_x \begin{pmatrix} \varrho v_x \\ \varrho v_x^2 + p \\ \varrho v_x v_y \\ (\varrho e + p)v_x \end{pmatrix}}_{=f^x(u)} + \underbrace{\partial_y \begin{pmatrix} \varrho v_y \\ \varrho v_x v_y \\ \varrho v_y^2 + p \\ (\varrho e + p)v_y \end{pmatrix}}_{=f^y(u)} = 0, \quad (59)$$

where  $\varrho$  is the density of the gas,  $v = (v_x, v_y)$  its speed,  $\varrho v$  the momentum,  $e$  the specific total energy, and  $p$  the pressure. The total energy  $\varrho e$  can be decomposed into the internal energy  $\varrho e$  and the kinetic energy  $E_{\text{kin}} = \frac{1}{2} \varrho v^2$ , i.e.  $\varrho e = \varrho e + \frac{1}{2} \varrho v^2$ . For a perfect gas,

$$p = (\gamma - 1) \varrho e = (\gamma - 1) \left( \varrho e - \frac{1}{2} \varrho v^2 \right), \quad (60)$$

where  $\gamma$  is the ratio of specific heats. For air,  $\gamma = 1.4$  will be used, unless stated otherwise.

Following [26, Section 7.4], the kinetic energy satisfies

$$-\partial_t E_{\text{kin}} = -\frac{1}{2} v^2 \partial_t \varrho + v \cdot \partial_t (\varrho v) = \partial_j \left( \frac{1}{2} \varrho v^2 v_j + p v_j \right) - p \partial_j v_j. \quad (61)$$

A numerical flux  $f^{\text{num},j}$  is *kinetic energy preserving*, if

$$f_{\varrho v_i}^{\text{num},j} = \{\!\{ v_i \}\!\} f_{\varrho}^{\text{num},j} + \{\!\{ p \}\!\} \delta_{ij}. \quad (62)$$

The corresponding numerical flux for the kinetic energy (approximating the conservative part of the kinetic energy equation) is [26, Eq. (7.66)]

$$F^{\text{num},j}(u^-, u^+) = \frac{1}{2} v_i^- v_i^+ f_\varrho^{\text{num},j}(u^-, u^+) + \frac{p^+ v_j^- + p^- v_j^+}{2}. \quad (63)$$

Using  $w = \partial_u E_{\text{kin}}(u)$ , a kinetic energy preserving semidiscretisation mimicking (61) has to satisfy (cf. [26, Section 7.4])

$$1^T M \partial_t E_{\text{kin}} = p^T M D_j v_j - 1^T R^T B N_j (F^{\text{num},j} - S^{\text{num},j}), \quad (64)$$

where the discretisation  $S^{\text{num},j}$  of the nonconservative term  $-p \partial_j v_j$  at the surface between two elements is given as

$$S^{\text{num},j}(u^-, u^+) = p^- \frac{v_j^+ - v_j^-}{2}. \quad (65)$$

Here, the argument  $u^-$  comes from the interior of an element and the argument  $u^+$  from the neighbouring element.

As mentioned in Remark 2.14, correction terms have been used to obtain kinetic energy preserving schemes in [34]. Contrary to the approach presented in the following, a certain split form of the Euler equations has been used there instead of a central discretisation and the correction terms are used to remove some interpolation errors at the boundaries.

Using the same approach as in Section 2.2 results in semidiscretisations (29), where the correction term  $r_i$  has to be chosen such that local conservation (27) and kinetic energy preservation (64) are satisfied.

**Remark 3.5.** Similarly to Remark 2.6, the constraints (27) and (64) do not contradict each other in a finite volume setting if kinetic energy preserving numerical surface fluxes  $f^{\text{num},j}$  are used, i.e. those satisfying (62).

The correction term for the kinetic energy is

$$\begin{aligned} r_i &= \alpha \left( w_i - \frac{1^T M w_i}{1^T M 1} \mathbf{1} \right), \quad \alpha = \frac{\mathcal{E}}{w_k^T M w_k - \frac{(1^T M w_k)(1^T M w_k)}{1^T M 1}}, \\ \mathcal{E} &= p^T M D_j v_j - 1^T R^T B N_j (F^{\text{num},j} - S^{\text{num},j}) - w_k^T M \text{VOL}_k - w_k^T M \text{SURF}_k. \end{aligned} \quad (66)$$

Similar to Theorem 2.7, one obtains

**Proposition 3.6.** *If the constraints (27) and (64) do not contradict each other, the correction term  $r$  (66) is the unique optimal correction of (29), measured in the discrete norm induced by  $M$ , such that (27) and (64) are satisfied.*

**Remark 3.7.** Using Theorem 3.3, combined correction terms for the entropy and kinetic energy can be created for the Euler equations. The corresponding entropy is chosen as

$$U = -\frac{\varrho s}{\gamma - 1}, \quad s = \log(p/\varrho^\gamma), \quad (67)$$

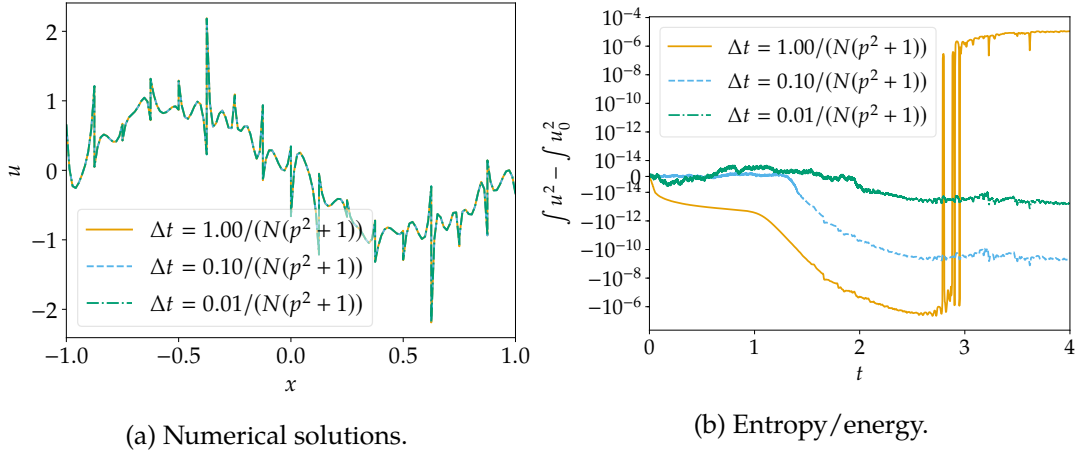


Figure 2: Numerical solutions of the linear advection equation and their energy/entropy, computed using a nodal DG scheme based on closed Newton Cotes quadrature.

the flux potentials are  $\psi^j = \varrho v_j$ , and the entropy variables are

$$w = U'(u) = \left( \frac{\gamma}{\gamma-1} - \frac{s}{\gamma-1} - \frac{\varrho v^2}{2p}, \frac{\varrho v_x}{p}, \frac{\varrho v_y}{p}, -\frac{\varrho}{p} \right)^T. \quad (68)$$

## 4 Numerical Examples

In this section, some numerical examples using the schemes described/derived hitherto will be presented.

### 4.1 Linear Advection

The linear advection equation

$$\begin{aligned} \partial_t u(t, x) + \partial_x u(t, x) &= 0, & x \in [-1, 1], t \in (0, 4), \\ u(0, x) &= u_0(x) = \sin(\pi x), & x \in [-1, 1], \end{aligned} \quad (69)$$

with periodic boundary conditions is solved numerically using a nodal DG scheme with  $N = 2^4$  uniform elements with polynomials of degree  $p = 4$  and closed Newton Cotes quadrature rules and the entropy correction is applied for the  $L^2$  entropy/energy  $U(u) = \frac{1}{2}u^2$ . The spatial semidiscretisation is integrated in time using SSPRK(10,4) of [21], which is energy stable for linear semidiscretisations [29].

Results of these simulations are visualised in Figure 2. Since the semidiscretisation is not linear because of the correction terms, the fully discrete scheme does not satisfy an entropy/energy inequality. However, the entropy/energy becomes constant to machine accuracy if the time step  $\Delta t$  is refined. Nevertheless, the numerical solutions are highly

oscillatory. While the entropy correction reduces the amount of oscillations compared to the numerical solution without correction (not shown), the basically bad behaviour of the nodal DG schemes with closed Newton Cotes quadrature can still be observed. It is no surprise that the quality of the solution depends crucially on the baseline scheme for such a quadratic optimisation approach. Additionally, this example demonstrates that an energy/entropy (in-)equality does not imply a good numerical approximation.

## 4.2 Two-Dimensional Scalar Equations

Here, the focus lies on a comparison between the correction terms (14) and (42) using different weightings. In (14), the identity matrix is used whereas (42) applies the mass matrix  $M$ . Here, a first comparison is given using these two approaches. It is clear that the difference will be quite small. However, to have a closer look on the behaviour two examples are demonstrated. Here, for the comparison a pure continuous Galerkin scheme in the RD framework [2] will be considered.

### 4.2.1 Rotation

The first problem is a linear rotation equation in two space dimensions given by

$$\begin{aligned} \partial_t u(t, x, y) + \partial_x(2\pi y u(t, x, y)) + \partial_y(2\pi x u(t, x, y)) &= 0, \quad (x, y) \in D, t \in (0, 1), \\ u(0, x, y) = u_0(x, y) &= \exp(-40(x^2 + (y - 0.5)^2)), \quad (x, y) \in D, \end{aligned} \quad (70)$$

where  $D$  is the unit disk in  $\mathbb{R}^2$ . For the boundary, outflow conditions will be considered. For time integration, the third order strong stability preserving scheme SSPRK(3,3) will be used with CFL number 0.2 and the correction in each step will be done. A pure continuous Galerkin scheme of third order is used and Bernstein polynomials are applied as basis functions. In this test, a small bump which is located around (0,0.5) is moving around in a circle. The rotation will be finished at  $t = 1$ . The mesh contains 3582 triangular elements. In Table (1), the change of the entropy

$$\int_{\Omega} U_{corr}^2(t) - \int_{\Omega} U_0^2 \quad (71)$$

is given after every 200 timesteps. In the second column, the correction term (14) is used to calculate the solution and (42) yields the results of the third column.

The differences in Table 1 are quite small and the correction terms lead in both cases to good results. It can also be realised that the entropy change oscillates around zero. For both correction terms, the errors of the numerical solutions are nearly identical. Using (14), the  $L_{\infty}$  error is given by 7.0158248661251754E-003. In the other case, one obtains 7.0158248660556755E-003. If we increase the number of DoFs (i.e. use more elements), the results are similar for this test case. The influence of the correction terms should be quite small for this smooth linear problem and the results support this supposition. Next, a non-linear equation will be considered.

Table 1: Total entropy change of numerical solutions using a continuous Galerkin scheme for the linear test problem (70).

Time	Correction (14)	Correction (42)
0.0924	-1.3200818722352396E-003	-1.3200818722352381E-003
0.1804	-3.5181442406824587E-003	-3.5181442406824587E-003
0.2707	-4.0384393285469204E-006	-4.0384393285469204E-006
0.3609	+1.6293437220984824E-006	+1.6293437220984879E-006
0.4512	+4.9053172644914367E-003	+4.9053172644914159E-003
0.5414	+4.9050945723263769E-003	+4.9050945723263708E-003
0.6317	+1.1157487764967766E-005	+1.1157487764967859E-005
0.7219	-1.5581264075219044E-006	-1.5581264075219041E-006
0.8122	-3.2331335892805870E-003	-3.2331335892805870E-003
0.9024	-2.3490459323906409E-003	-2.3490459323906449E-003
0.9927	-5.3314892415756020E-006	-5.3314892416167162E-006
1.0000	-5.3476245962391514E-006	-5.3476245962789874E-006

#### 4.2.2 Burgers' Type of Equation

The problem is given by

$$\begin{aligned} \partial_t u(t, x, y) + \partial_x(\cos u(t, x, y)) + \partial_y u(t, x, y) &= 0, \quad (x, y) \in D, t \in (0, 0.2) \\ u(0, x, y) = u_0(x, y) &= \exp(-40(x^2 + y^2)), \quad (x, y) \in D, \end{aligned} \quad (72)$$

where  $D$  is the unit disk in  $\mathbb{R}^2$ . Again, outflow boundary conditions will be considered and time integration is done via SSPRK(3,3) with CFL number 0.1. The space discretisation is again done by a pure continuous Galerkin scheme of third order with Bernstein polynomials. In this test case, a small bump located around zero will move up to the left and a shock will appear after a finite time. However, for this study, the time is considered before the shock appears. The choice of  $\cos$  in (72) is done on purpose to guarantee that the integration with a quadrature rule will never be exact. The influence of the different correction terms is not visible in the solution in Figure 3, where the solution at  $t = 0.2$  (right before the shock appears) is visualised.

Here, the correction (42) is applied. For the square entropy  $U = u^2/2$ , the differences  $\int_{\Omega} U_{corr}^2(0.2) - \int_{\Omega} U_0^2$  of the entropies with the different corrections are

- 4.3760551889451007E-006 for the correction (14) and
- 4.3739395943294535E-006 for the correction (42)

at  $t = 0.2$ . The difference between the influence of the correction terms is also quite small for this test case.

**Remark 4.1.** Several simulations (also with other test problems such as Burgers' equation) have been performed. Up to now, no significant difference between the two

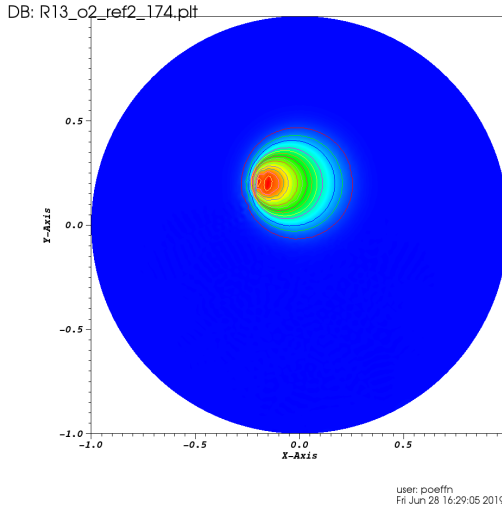


Figure 3: Bump at the time  $t = 0.2$  calculated with 7052 triangles and a continuous Galerkin scheme.

correction terms has been seen for Galerkin schemes. However, the possibility of some advantages of one of the correction terms compared to the other one cannot be excluded at the present time (e.g. in a different scheme or for other problems). Further studies have to be conducted.

### 4.3 Euler Equations

A Taylor-Green vortex initial condition for the compressible Euler equations given by

$$\begin{aligned} \varrho(0, x, y) &= 1, & v_x(0, x, y) &= \sin(x) \cos(y), \\ v_y(0, x, y) &= -\cos(x) \sin(y), & p(0, x, y) &= \frac{100}{\gamma} + \frac{\cos(2x) + \cos(2y)}{4}, \end{aligned} \quad (73)$$

for  $(x, y) \in [0, 2\pi]^2$  with periodic boundary conditions is considered, which is a stationary solution of the incompressible Euler equations. Using classical sixth order central finite difference operators with 100 nodes per coordinate direction, the numerical solutions have been computed in the time interval  $t \in [0, 30]$  with the fourth order, ten-stage, strong stability preserving Runge-Kutta method of [21] and a constant time step  $\Delta t = \Delta x/8$ .

The relative kinetic energy and entropy of numerical solutions obtained via the classical central scheme with or without corrections or flux difference schemes are visualised in Figure 4. The classical central scheme blows up at  $t \approx 23.50$  and strong variations of both the kinetic energy and the entropy can be observed shortly before. Using a correction term for the kinetic energy reduces the variations of  $E_{\text{kin}}$  before the blow-up slightly and does not influence the entropy significantly before  $t \approx 20$ . However, the scheme blows up at approximately the same time.

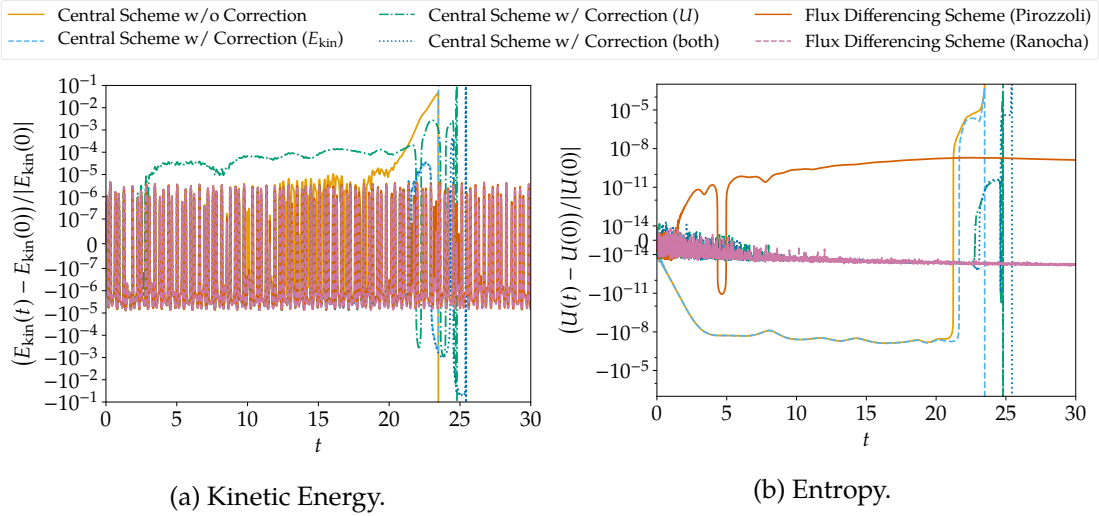


Figure 4: Relative kinetic energy  $E_{\text{kin}}$  and entropy  $U$  of numerical solutions of the compressible Euler equations with a Taylor-Green vortex initial condition. The finite difference schemes use sixth order classical central stencils and either the classical central scheme with or without correction term or flux difference schemes with numerical fluxes of [25] (see also [19]) or [26, Theorem 7.8].

Using instead a correction term for the entropy, the scheme crashes a bit later at  $t \approx 24.82$ . This correction term results in an increase of the kinetic energy in this case. The entropy remains constant until it starts to vary before the blow-up. Applying the combined correction term for both entropy and kinetic energy yields to some extent combined results: The oscillations of the kinetic energy are very similar to those with the  $E_{\text{kin}}$  correction and the entropy develops similarly to the one using only the  $U$  correction. However, the scheme using the combined correction term crashes a bit later ( $t \approx 25.46$ ) than the other ones.

Substituting the central scheme with a non-trivial flux difference discretisation can improve the numerical stability significantly. The numerical fluxes of Pirozzoli [25] (see also [19]) and Ranocha [26, Theorem 7.8] are kinetic energy preserving, i.e. they satisfy (64) analytically. The last flux is also entropy conservative, i.e. the corresponding scheme satisfies (28). The flux difference scheme does not crash during the computation if either one of these fluxes is used. Both show some oscillations of the kinetic energy with an amplitude similar to the central scheme with  $E_{\text{kin}}$  correction. The entropy varies in time if Pirozzoli's flux is used and the amount of variation is similar to the one for the central scheme before the blow-up. Remarkably, the scheme using the flux of [26, Theorem 7.8] and the central schemes with entropy correction conserve the entropy nearly to machine accuracy. This can not necessarily be expected, since the scheme is only semidiscretely entropy conservative and the time integration scheme can (and will typically) cause variations of  $U$ .

Additionally, a nodal discontinuous Galerkin scheme on Lobatto Legendre nodes

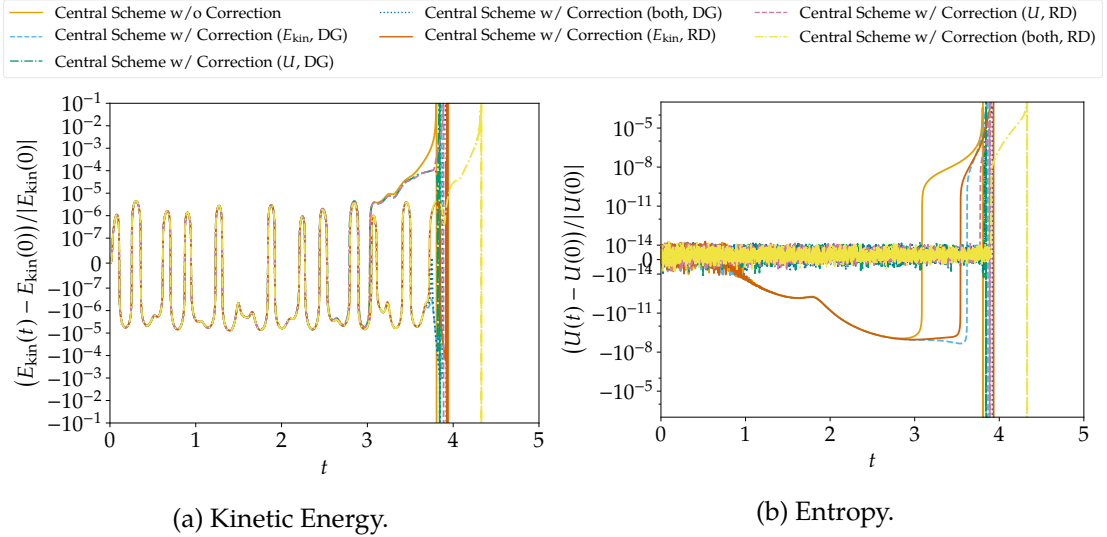


Figure 5: Relative kinetic energy  $E_{\text{kin}}$  and entropy  $U$  of numerical solutions of the compressible Euler equations with a Taylor-Green vortex initial condition. The nodal discontinuous Galerkin schemes use polynomials of degree  $p = 5$  on Lobatto Legendre nodes, a classical central scheme in the interior of each element, and the numerical fluxes of [26, Theorem 7.8] between elements.

with polynomial degree  $p = 5$  and 16 elements per coordinate direction has been used. The numerical flux at the boundaries is the one of [26, Theorem 7.8] and the classical central scheme is used in the interior of each element. The numerical solutions have been integrated in time with the fourth order, ten-stage, strong stability preserving Runge-Kutta method of [21] and a constant time step  $\Delta t = \frac{\Delta x}{10} \frac{1}{p^2+1}$ , where  $\Delta x$  is the width of one element.

The trend of the results is very similar to the case of finite difference methods described before: Using the central scheme in the interior of each element results in a blow-up (that happens before the corresponding one for the FD scheme) at  $t \approx 3.8$ . Applying a correction for  $E_{\text{kin}}$  removes the increase of the kinetic energy before the blow-up and applying a correction for  $U$  yields a nearly constant entropy (before the blow-up).

In general, there does not seem to be a big difference between the basic choices for the correction terms (14) and (30). The different weighting does not seem to be crucial for these unstable calculations here. The only minor exception is the correction term for both  $E_{\text{kin}}$  and  $U$  with a weighting as in (14), which blows up slightly later at  $t \approx 4.3$ .

The computations using flux differencing schemes in the interior of each element analogously to the finite difference schemes remain stable and do not blow up in this test case, contrary to the central scheme with correction terms. Moreover, applying corrections to a flux difference scheme based on the flux of Pirozzoli [25] yields results that are very similar to the scheme using the flux of Ranocha [26, Theorem 7.8] (not shown in the plot). In particular, the entropy can be conserved and the numerical

solutions does not blow up during the computation.

#### 4.4 Convergence Test

Here, a convergence test using the initial condition

$$\begin{aligned}\varrho(0, x, y) &= 1 + \frac{1}{2} \sin(\pi x), & v_x(0, x, y) &= 1, \\ v_y(0, x, y) &= 0, & p(0, x, y) &= 1,\end{aligned}\tag{74}$$

for the Euler equations (59) in the periodic domain  $[0, 2] \times [0, 1]$  using DG schemes is conducted using  $N_x$  elements in  $x$  direction,  $N_y = 1$  element in  $y$  direction, and polynomials of degree  $p = 4$ . The error of the density at the final time  $t = 6$  is computed using the Lobatto Legendre quadrature. As can be seen in Table 2, there are no significant differences between the baseline central scheme and the ones applying a correction term, in accordance with results of [2]. For low resolutions, the correction term (42) using a weighting by the mass matrix yields slightly lower errors than the one proposed originally in [2].

Table 2: Convergence rates for central and corrected DG schemes using polynomials of degree  $p = 4$  for the Euler equations with initial condition (74).

$N_x$	Central Scheme		Correction (42)		Correction (14)	
	$\ \varrho - \varrho_0\ _M$	EOC	$\ \varrho - \varrho_0\ _M$	EOC	$\ \varrho - \varrho_0\ _M$	EOC
5	1.312e-05		1.025e-04		2.537e-04	
10	1.394e-06	+3.23	1.994e-06	+5.68	3.041e-06	+6.38
15	3.095e-07	+3.71	3.217e-07	+4.50	3.436e-07	+5.38
20	6.426e-08	+5.46	6.486e-08	+5.57	6.714e-08	+5.68
25	1.810e-08	+5.68	1.819e-08	+5.70	1.836e-08	+5.81

## 5 Applications to Grid Refinement and Coarsening

There is a certain interest in spatial adaptivity for entropy conservative and dissipative semidiscretisations [15, 17]. If such adaptive schemes shall also be adapted in time, grid refinement and coarsening operators transferring the numerical approximation from one grid to another have to be constructed. Ideally, these should respect the entropy dissipative behavior, which is not fulfilled by e.g. the classical  $L^2$  projection used for such operations.

Consider a fine grid  $\Omega_f$  and a coarse grid  $\Omega_c$ . In the following, it will be assumed that a nodal discontinuous element type basis is used and that there are associated interpolation operators  $I_{f \leftarrow c}$  from the coarse to the fine grid and  $I_{c \leftarrow f}$  from the fine grid to the coarse grid. Numerical solutions and operators on the coarse/fine grid will be written using upper indices  $c/f$ .

While standard interpolation and  $L^2$  projection operators conserve the total mass for reasonable choices of the basis functions and quadrature rule, it is in general impossible to obtain strict inequalities for entropies. Hence, it is of interest to apply an optimisation approach similar to the one described in the previous section.

However, there are important differences concerning the optimisation approach to entropy dissipativity between computations of spatial semidiscretisations and refinement/coarsening operators:

- Computing the time derivative of the entropy results in a linearisation of the problem, making it much easier. In fact, a closed solution is given in the previous sections. For the refinement/coarsening operators, such a closed form solution does not seem to be available in general.
- The spatial semidiscretisation has to be evaluated for every element and every time step, possibly multiple times. Contrary, the refinement/coarsening operators will be evaluated significantly fewer times.

To sum up, entropy stable refinement/coarsening operators are more expensive but also used less often. Hence, they can be of interest in applications requiring strict entropy inequalities.

## 5.1 Refinement

Given a solution  $u^c$  on the coarse grid, an optimisation problem for the solution  $u^f$  on the fine grid is

$$\begin{aligned} & \min_{u^f} \frac{1}{2} \|u^f - I_{f \leftarrow c} u^c\|_{M^f}^2 \\ \text{s. t. } & 1^T M^f u^f = 1^T M^c u^c, \quad 1^T M^f U(u^f) \leq 1^T M^c U(u^c). \end{aligned} \quad (75)$$

Since the norm  $\|\cdot\|_{M^f}$  is strictly convex & coercive and the entropy  $U$  is convex, there exists a unique solution of (75). This convex problem can be solved using standard constrained optimisation algorithms. For the numerical examples presented below, Ipopt [39] has been used via the interface provided by JuMP [11].

After some simplifications, the first order necessary condition becomes [24, Theorem 12.1]

$$u^f = I_{f \leftarrow c} u^c + \lambda \left( w(u^f) - \frac{1^T M^f w(u^f)}{1^T M^f 1} 1 \right), \quad (76)$$

where  $\lambda \geq 0$  is a Lagrange multiplier. Assuming that  $I_{f \leftarrow c} u^c$  is already a good approximation to  $u^f$ ,  $w(u^f)$  can be substituted by  $w(I_{f \leftarrow c} u^c)$ , resulting in the simpler problem

$$\begin{aligned} & \min_{\lambda} \frac{1}{2} \lambda^2 \\ \text{s. t. } & 1^T M^f U \left( I_{f \leftarrow c} u^c + \lambda \left( w(I_{f \leftarrow c} u^c) - \frac{1^T M^f w(I_{f \leftarrow c} u^c)}{1^T M^f 1} 1 \right) \right) \leq 1^T M^c U(u^c). \end{aligned} \quad (77)$$

## 5.2 Coarsening

For a solution  $u^f$  on the fine grid, an optimisation problem for the solution  $u^c$  on the coarse grid is

$$\begin{aligned} \min_{u^c} \frac{1}{2} \left\| I_{f \leftarrow c} u^c - u^f \right\|_{M^f}^2 \\ \text{s. t. } 1^T M^c u^c = 1^T M^f u^f, \quad 1^T M^c U(u^c) \leq 1^T M^f U(u^f). \end{aligned} \quad (78)$$

This is again a convex optimisation problem possessing a unique solution.

## 5.3 Numerical Examples

Consider the interval  $[-1, 1]$  with Lobatto-Legendre nodes for polynomials of degree  $\leq 6$  on the fine grid and  $\leq 3$  on the coarse grid. The interpolation operators are given by polynomial interpolation and the mass matrices as diagonal matrices using the weights of the corresponding quadrature rule. The exponential entropy  $U(u) = \exp(u)$  is used in the following.

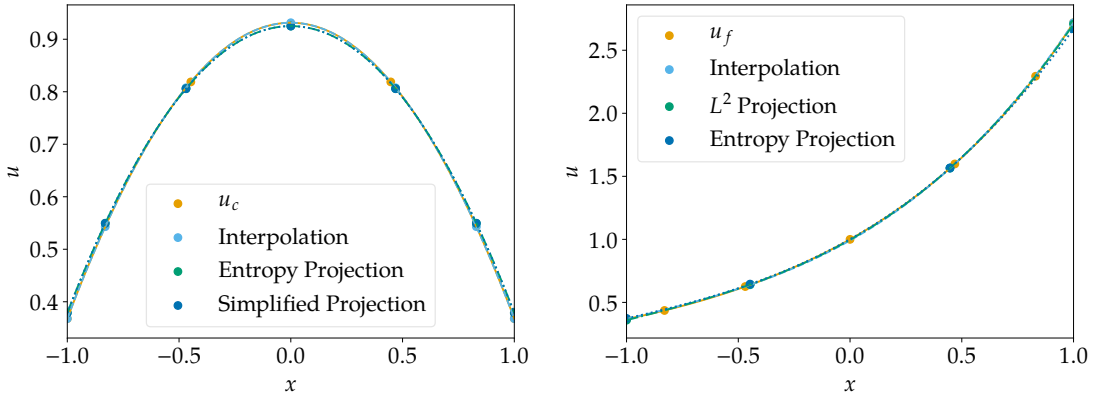
For the refinement experiment in Figure 6a, the solution on the coarse grid is obtained by evaluating  $\exp(-x^2)$  on the coarse grid. While the standard interpolation produces spurious entropy, both optimisation approaches satisfy the entropy inequality up to the tolerances specified for the algorithms. The optimisation results are visually indistinguishable and slightly dissipated compared to the interpolant.

The coarsening experiment presented in Figure 6b is initialised by evaluating  $\exp(x)$  on the fine grid. Both the interpolation and standard  $L^2$  projection produce spurious amounts of entropy. Contrary, the result obtained by optimisation (78) satisfies the desired entropy inequality.

## 6 Summary and Conclusions

In this paper, a reinterpretation and extension of entropy correction terms developed/proposed in [2] is given. Based on a characterisation of these terms as solutions of certain optimisation problems, different correction terms are determined by the choice of discrete norms. Additionally, these terms are adapted to numerical methods such as discontinuous Galerkin and finite difference schemes. In numerical simulations, the various correction terms are tested and compared also to flux difference approaches [14, 19]. These tests demonstrate that there is no significant difference between the two basic choices of correction terms (given in (14) and (41), respectively).

However, using a flux difference formulation shows advantages compared to the application of these corrections terms to a central scheme. While the correction terms work and preserve the kinetic energy and/or conserve the entropy for the Euler equations as expected, they cannot prevent a blow-up of numerical solutions for a demanding Taylor-Green vortex type initial condition. If a flux difference scheme is used as baseline scheme that is not entropy conservative, the correction terms can be applied successfully,



(a) Refinement. The spurious entropy production of the interpolation is  $+3.566e-03$ , the optimisation approach (75) yields a slight entropy decay of  $-3.980e-08$  and the simplified problem (77) results in  $+2.497e-08$ . Both optimisation results deviate from the interpolation by  $+7.562e-03$ .

(b) Coarsening. The spurious entropy production of the interpolation is  $+9.749e-02$ , the amount of entropy produced by the  $L^2$  projection is  $+7.767e-02$ , and the optimisation approach results in a slight entropy decay of  $-3.429e-07$ .

Figure 6:  $p$  refinement and coarsening using polynomials of degree  $\leq 6$  on the fine grid and of degree  $\leq 3$  on the coarse grid with exponential entropy  $U(u) = \exp(u)$ .

yielding an entropy conservative scheme that does not blow up during the computation. This can be interpreted as follows: Firstly, the correction terms cannot “fix a baseline scheme magically”; if the scheme without correction is too bad (such as a central scheme in these test cases), the corrections work but cannot prevent a blow-up due to negative density/pressure. Secondly, the success of flux difference schemes cannot be attributed solely to resulting equations for the kinetic energy or entropy across elements. Inter-element/subcell local equations (which hold for these schemes) might play a role for the improved numerical stability.

Nevertheless, the flux difference framework includes some assumptions on the quadrature, i.e. summation by parts (SBP) property as discrete analogue of integration by parts. The application of the correction terms does not need these assumptions. Hence, it is more general. In particular, it can be applied to members of the framework of residual distribution schemes. However, these experiments are only a first comparison. Further tests have to be done in this direction but this is not topic of this current paper.

Besides the reinterpretation of the correction terms, their extension to new applications has been conducted. Here, novel generalisations to entropy inequalities, multiple constraints, and kinetic energy preservation for the Euler equations are developed and verified by numerical simulations with a focus on multiple constraints such as conserving the entropy and preserving the kinetic energy simultaneously. Finally, the idea of such an optimisation approach is applied to grid refinement processes and coarsening operators. An entropy stable/dissipative grid transfer is demonstrated analytically

and numerically.

## Acknowledgements

The second author has been funded by the SNF project (Number 175784) and the UZH Postdoc Scholarship. The third author was supported by the German Research Foundation (DFG, Deutsche Forschungsgemeinschaft) under Grant SO 363/14-1.

## References

- [1] R. Abgrall. 'High order schemes for hyperbolic problems using globally continuous approximation and avoiding mass matrices'. In: *Journal of Scientific Computing* 73.2-3 (2017), pp. 461–494.
- [2] R. Abgrall. 'A general framework to construct schemes satisfying additional conservation relations. Application to entropy conservative and entropy dissipative schemes'. In: *Journal of Computational Physics* 372 (2018), pp. 640–666. doi: [10.1016/j.jcp.2018.06.031](https://doi.org/10.1016/j.jcp.2018.06.031). arXiv: [1711.10358](https://arxiv.org/abs/1711.10358) [math.NA].
- [3] R. Abgrall, P. Bacigaluppi and S. Tokareva. 'A high-order nonconservative approach for hyperbolic equations in fluid dynamics'. In: *Computers & Fluids* 19.1-3 (2017).
- [4] R. Abgrall, A. Larat and M. Ricchiuto. 'Construction of very high order residual distribution schemes for steady inviscid flow problems on hybrid unstructured meshes'. In: *Journal of Computational Physics* 230.11 (2011), pp. 4103–4136.
- [5] R. Abgrall, E. I. Meledo and P. Oeffner. 'On the Connection between Residual Distribution Schemes and Flux Reconstruction'. In: *arXiv preprint arXiv:1807.01261* (2018).
- [6] R. Abgrall and P. L. Roe. 'High order fluctuation schemes on triangular meshes'. In: *Journal of Scientific Computing* 19.1-3 (2003), pp. 3–36.
- [7] M. Bohm, A. R. Winters, G. J. Gassner, D. Derigs, F. Hindenlang and J. Saur. 'An entropy stable nodal discontinuous Galerkin method for the resistive MHD equations. Part I: Theory and Numerical Verification'. In: *Journal of Computational Physics* (2018). doi: [10.1016/j.jcp.2018.06.027](https://doi.org/10.1016/j.jcp.2018.06.027).
- [8] M. H. Carpenter, M. Parsani, T. C. Fisher and E. J. Nielsen. 'Towards an entropy stable spectral element framework for computational fluid dynamics'. In: *54th AIAA Aerospace Sciences Meeting*. American Institute of Aeronautics and Astronautics. 2016. doi: [10.2514/6.2016-1058](https://doi.org/10.2514/6.2016-1058).
- [9] J. Chan. 'On discretely entropy conservative and entropy stable discontinuous Galerkin methods'. In: *Journal of Computational Physics* 362 (2018), pp. 346–374. doi: [10.1016/j.jcp.2018.02.033](https://doi.org/10.1016/j.jcp.2018.02.033).

- [10] C. M. Dafermos. *Hyperbolic Conservation Laws in Continuum Physics*. Berlin Heidelberg: Springer-Verlag, 2010. doi: [10.1007/978-3-642-04048-1](https://doi.org/10.1007/978-3-642-04048-1).
- [11] I. Dunning, J. Huchette and M. Lubin. 'JuMP: A Modeling Language for Mathematical Optimization'. In: *SIAM Review* 59.2 (2017), pp. 295–320. doi: [10.1137/15M1020575](https://doi.org/10.1137/15M1020575).
- [12] D. C. D. R. Fernández, P. D. Boom and D. W. Zingg. 'A generalized framework for nodal first derivative summation-by-parts operators'. In: *Journal of Computational Physics* 266 (2014), pp. 214–239. doi: [10.1016/j.jcp.2014.01.038](https://doi.org/10.1016/j.jcp.2014.01.038).
- [13] D. C. D. R. Fernández, J. E. Hicken and D. W. Zingg. 'Review of summation-by-parts operators with simultaneous approximation terms for the numerical solution of partial differential equations'. In: *Computers & Fluids* 95 (2014), pp. 171–196. doi: [10.1016/j.compfluid.2014.02.016](https://doi.org/10.1016/j.compfluid.2014.02.016).
- [14] T. C. Fisher and M. H. Carpenter. 'High-order entropy stable finite difference schemes for nonlinear conservation laws: Finite domains'. In: *Journal of Computational Physics* 252 (2013), pp. 518–557. doi: [10.1016/j.jcp.2013.06.014](https://doi.org/10.1016/j.jcp.2013.06.014).
- [15] L. Friedrich, D. C. D. R. Fernández, A. R. Winters, G. J. Gassner, D. W. Zingg and J. Hicken. 'Conservative and stable degree preserving SBP operators for non-conforming meshes'. In: *Journal of Scientific Computing* (2018), pp. 1–30. doi: [10.1007/s10915-017-0563-z](https://doi.org/10.1007/s10915-017-0563-z).
- [16] L. Friedrich, G. Schnücke, A. R. Winters, D. C. D. R. Fernández, G. J. Gassner and M. H. Carpenter. 'Entropy Stable Space-Time Discontinuous Galerkin Schemes with Summation-by-Parts Property for Hyperbolic Conservation Laws'. In: *Journal of Scientific Computing* (2018), pp. 1–48. doi: [10.1007/s10915-019-00933-2](https://doi.org/10.1007/s10915-019-00933-2). arXiv: [1808.08218](https://arxiv.org/abs/1808.08218) [math.NA].
- [17] L. Friedrich, A. R. Winters, D. C. D. R. Fernández, G. J. Gassner, M. Parsani and M. H. Carpenter. 'An entropy stable h/p non-conforming discontinuous Galerkin method with the summation-by-parts property'. In: *Journal of Scientific Computing* 77.2 (2018), pp. 689–725. doi: [10.1007/s10915-018-0733-7](https://doi.org/10.1007/s10915-018-0733-7).
- [18] G. J. Gassner. 'A Skew-Symmetric Discontinuous Galerkin Spectral Element Discretization and Its Relation to SBP-SAT Finite Difference Methods'. In: *SIAM Journal on Scientific Computing* 35.3 (2013), A1233–A1253. doi: [10.1137/120890144](https://doi.org/10.1137/120890144).
- [19] G. J. Gassner, A. R. Winters and D. A. Kopriva. 'Split Form Nodal Discontinuous Galerkin Schemes with Summation-By-Parts Property for the Compressible Euler Equations'. In: *Journal of Computational Physics* 327 (2016), pp. 39–66. doi: [10.1016/j.jcp.2016.09.013](https://doi.org/10.1016/j.jcp.2016.09.013).
- [20] J. E. Hicken and J. Crean. *A Family of Entropy-Conservative Flux Functions for the Euler Equations*. 2018. arXiv: [1807.03832](https://arxiv.org/abs/1807.03832) [math.NA].
- [21] D. I. Ketcheson. 'Highly Efficient Strong Stability-Preserving Runge-Kutta Methods with Low-Storage Implementations'. In: *SIAM Journal on Scientific Computing* 30.4 (2008), pp. 2113–2136. doi: [10.1137/07070485X](https://doi.org/10.1137/07070485X).

- [22] D. I. Ketcheson. *Relaxation Runge–Kutta Methods: Conservation and Stability for Inner-Product Norms*. May 2019. arXiv: 1905.09847 [math.NA].
- [23] R.-H. Ni. ‘A multiple grid scheme for solving the Euler equations’. In: *5th Computational Fluid Dynamics Conference*. 1981, p. 1025.
- [24] J. Nocedal and S. J. Wright. *Numerical Optimization*. New York: Springer-Verlag, 1999.
- [25] S. Pirozzoli. ‘Numerical Methods for High-Speed Flows’. In: *Annual Review of Fluid Mechanics* 43 (2011), pp. 163–194. doi: 10.1146/annurev-fluid-122109-160718.
- [26] H. Ranocha. ‘Generalised Summation-by-Parts Operators and Entropy Stability of Numerical Methods for Hyperbolic Balance Laws’. PhD thesis. TU Braunschweig, Feb. 2018.
- [27] H. Ranocha. *On Strong Stability of Explicit Runge-Kutta Methods for Nonlinear Semi-bounded Operators*. Nov. 2018. arXiv: 1811.11601 [math.NA].
- [28] H. Ranocha. ‘Shallow water equations: Split-form, entropy stable, well-balanced, and positivity preserving numerical methods’. In: *GEM – International Journal on Geomathematics* 8.1 (Apr. 2017), pp. 85–133. doi: 10.1007/s13137-016-0089-9. arXiv: 1609.08029 [math.NA].
- [29] H. Ranocha and P. Öffner. ‘ $L_2$  Stability of Explicit Runge-Kutta Schemes’. In: *Journal of Scientific Computing* 75.2 (May 2018), pp. 1040–1056. doi: 10.1007/s10915-017-0595-4.
- [30] H. Ranocha, K. Ostaszewski and P. Heinisch. *Numerical Methods for the Magnetic Induction Equation with Hall Effect and Projections onto Divergence-Free Vector Fields*. Submitted. Oct. 2018. arXiv: 1810.01397 [math.NA].
- [31] H. Ranocha, M. Sayyari, L. Dalcin, M. Parsani and D. I. Ketcheson. *Relaxation Runge–Kutta Methods: Fully-Discrete Explicit Entropy-Stable Schemes for the Euler and Navier–Stokes Equations*. May 2019. arXiv: 1905.09129 [math.NA].
- [32] M. Ricchiuto and R. Abgrall. ‘Explicit Runge–Kutta residual distribution schemes for time dependent problems: second order case’. In: *Journal of Computational Physics* 229.16 (2010), pp. 5653–5691.
- [33] P. L. Roe. ‘Approximate Riemann solvers, parameter vectors, and difference schemes’. In: *Journal of Computational Physics* 43.2 (1981), pp. 357–372. doi: 10.1016/0021-9991(81)90128-5.
- [34] V. Singh and S. Frankel. *Kinetic energy preserving split form flux reconstruction for the compressible Euler equations at Gauss nodes*. Talk presented at the European Workshop on High Order Nonlinear Numerical Methods for Evolutionary PDEs: Theory and Applications (HONOM). Madrid, 2019.
- [35] B. Sjögreen and H. Yee. ‘High order entropy conservative central schemes for wide ranges of compressible gas dynamics and MHD flows’. In: *Journal of Computational Physics* 364 (2018), pp. 153–185. doi: 10.1016/j.jcp.2018.02.003.

- [36] M. Svärd and J. Nordström. 'Review of summation-by-parts schemes for initial-boundary-value problems'. In: *Journal of Computational Physics* 268 (2014), pp. 17–38. doi: [10.1016/j.jcp.2014.02.031](https://doi.org/10.1016/j.jcp.2014.02.031).
- [37] E. Tadmor. 'Entropy stability theory for difference approximations of nonlinear conservation laws and related time-dependent problems'. In: *Acta Numerica* 12 (2003), pp. 451–512. doi: [10.1017/S0962492902000156](https://doi.org/10.1017/S0962492902000156).
- [38] E. Tadmor. 'The numerical viscosity of entropy stable schemes for systems of conservation laws. I'. In: *Mathematics of Computation* 49.179 (1987), pp. 91–103. doi: [10.1090/S0025-5718-1987-0890255-3](https://doi.org/10.1090/S0025-5718-1987-0890255-3).
- [39] A. Wächter and L. T. Biegler. 'On the implementation of an interior-point filter line-search algorithm for large-scale nonlinear programming'. In: *Mathematical Programming* 106.1 (2006), pp. 25–57. doi: [10.1007/s10107-004-0559-y](https://doi.org/10.1007/s10107-004-0559-y).
- [40] N. Wintermeyer, A. R. Winters, G. J. Gassner and D. A. Kopriva. 'An entropy stable nodal discontinuous Galerkin method for the two dimensional shallow water equations on unstructured curvilinear meshes with discontinuous bathymetry'. In: *Journal of Computational Physics* 340 (2017), pp. 200–242. doi: [10.1016/j.jcp.2017.03.036](https://doi.org/10.1016/j.jcp.2017.03.036).